

Parallel, hybrid KD tree and geometry level set method for simulating ship hydrodynamics using unstructured dynamic overset grid

HUANG Jun-tao

(OHMUGA Fluid Dynamics Inc., St. John's, NL, Canada, A1A 1Z4. Email: jhuang@ohmuga.com)

Abstract: A parallel, hybrid KD tree search and geometry method is advised for CFD-OHMUGA for calculating close points for level set reinitialization for ship hydrodynamics with motions in unstructured dynamic overset grids. The aim is to resolve the difficulties of keeping accuracy and robust for level set reinitialization in non-orthogonal curvilinear structured grids or unstructured grids. In this method, positions of free surface points are calculated at first, efficient KD tree search is then performed to choose three best free surface points following the constraints of the smallest distance to tagged point and the closest three orthogonal axis created recursively, finally the level set values at close points are calculated from those three points using geometry method. MPI parallel method is also advised to make the process more efficiently by extending the fiction region of the free surface points from other related processors. Unstructured dynamic overset grid solver named Overset-OHMUGA is coupled to solve the problems of complicated geometries, relative body motions, and local grid refinements. Validations show that computational results have good agreements with the experimental data. An example of course keeping is also demonstrated including autopilot, controllers, and 6DOF motions in irregular waves.

Key words: Unstructured dynamic overset grid; Free surface; Level set method; Parallel KD tree and geometry method; Ship hydrodynamics.

1 Introduction

Level set method (Osher and Sethian^[1], Sussman et al.^[2]) is a surface capture method for simulating viscous moving interface or free surface flow of ship hydrodynamics (Huang et al.^[3-4],

Huang^[5], Stern et al.^[6-7], Vukcevic et al.^[8]). Level set reinitialization is always required to keep distance function. The reinitialization is usually classified as two methods, one is full-field derivative method advised by Sussman et al.^[2], which however faces challenges to keep efficiency in the condition of very skew grids of such as non-orthogonal structured grids or unstructured grid (Huang^[5]). Another is an efficient method named as close point based method, where the close points are first calculated, then level set looks close points as computational boundaries and its values in far field are solved either by fast marching (Sethian^[9]) method or derivative equation (Carrica et al.^[10]). As for close point based method, the important and first step is how to calculate level set values at close points locating at grid nodes, which are calculated from the position information of free surface points around them. As introduced by Sethian^[9], level set value at a tagged close point is calculated as distance to a plane constructed by the closest three (two or one if not available) free surface points on corresponding three orthogonal coordinates. Carrica et al.^[10], extend this method to the curvilinear structured grid, however, it is still a challenge to keep accurate and robust in very skew non-orthogonal grids. The situation is even more difficult for unstructured grid, since the points of free surface are dispersive and irregular and also there are not three coordinates to rely on.

In order to resolve the above difficulties, in this paper, we provide a parallel, hybrid KD tree search and geometry method to reinitialize the level set values at close points for non-orthogonal structured grids and unstructured grids. Validations and demonstrations for ship hydrodynamics are performed considering the situations of free surface flow, ship autopilot, controllers, 1-6 DOF motions, incoming linear regular or irregular waves, etc.

2 Mathematical model

CFD-OHMUGA (Huang^[5,11-12]) is a parallel, unstructured, dynamic overset grid (coupled with Overset-OHMUGA, Huang^[13]), viscous turbulence flow solver, which is designed for simulating wave and multi-body (or flow and multi-body) interactions with 6DOF body motions in marine hydrodynamics (e.g. ship resistance, maneuvering and seakeeping). The free surface is modeled with a single-phase capturing method used for predicting arbitrary interface topology changes, where only the water flow is solved, enforcing interface physical conditions. It uses either dynamic overset multi-block structured (transform to unstructured grid automatically) or unstructured grids being compatible to very complicated physical geometries and relative body motions. Capabilities include RANS/DES turbulence models, incoming regular or irregular waves (considering dispersion relationship of water depth), prescribed or predicted (captive or free) rigid multi-body 6DOF motions, propulsion models, controllers for speed and heading

(3DOF independent rotation motions from body, appendage or model, open-loop or feed-back method), linear mooring model, and so on.

3 Numerical methods

In current work, finite volume methods are adopted for all governing equations in the dual control volume centered by element-vertex and constructed from tetrahedral, hexahedral, prismatic or pyramid elements, PISO or projection method are applied for the velocity and pressure coupling, isoparametric method is advised to discretize the pressure Poisson equation, 2nd-order implicit method is used for temporal and spatial discretization for momentum and level set governing equation, limiter functions are adopted for convection term discretization (Venkatakrishnan or Barth Jesperson limiter, or TVD method of Roe's minmod, Roe's superbee, van Albada, Van Leer, etc.), narrow band and geometry method is provided for level set equations, and implicit 2nd-order method is used for rigid body dynamic equations. Note of that dynamic overset grid technique is implemented by using Overset-OHMUGA with ALE technique (Arbitrary Lagrangian Eulerian method), where Overset-OHMUGA is an independent, fully MPI parallel, unstructured, overset grid solver, who couples with CFD solvers by files (static) or MPI interface (dynamic), and provides DCI (Domain Connectivity Information) and surface area weight coefficients serving for different CFD solvers^[5,11-13].

A hybrid KD tree fast search and geometry method, and derivative equation method is adopted for level set reinitialization. The KD tree fast search and geometry method is used to calculate the distance for the close points (with a neighbor point on the other side of free surface), and the derivative equation is used to solve the rest parts looking the close points as computational boundaries, and communicating information from free surface to the far regions.

In our method, data structure of KD tree (Bentley^[14]), a multidimensional binary tree, which is utilized here to search the nearest-neighbor point necessary. The main task is to find a point which is the closest to a tagged point with some special constraints.

Studying from Sethian's method^[9] applied in orthogonal grid, the current method tries to approximate the orthogonal coordinate method as possible as it can.

Step 1, we should set all the free surface points, by using the position interpolation between close points as following

$$\mathbf{X}_I = [(1-\lambda)\mathbf{X}_P + \lambda\mathbf{X}_Q] \quad (1)$$

where $\lambda = \varphi_P / (\varphi_P - \varphi_Q)$ is ratio calculated by the level set values. Note of that P is tagged point, Q is

another point in other fluid, and point p and Q are two end points of an edge.

For parallel computation, an extended bounding box including fiction region and necessary information in other related processors is required. Thus, we have enough information to calculate the distance to free surface for all close points in current processor. Following Fig. 1, we are going to handle a close point P in water who has some free surface points nearby. Assume the dark circle points are free surface points (A,B,C,Q1,Q2,Q3,Q4,Q5,...), which have irregular 3D distributions all of the computational domain.

Step 2, Create a KD tree by inserting all free surface into the data structure.

Step 3, find a closest free surface point A to point P, and found the first coordinate with the direction of \overrightarrow{PA} .

Step 4. Found a plane named plane1 in Fig.1 which is perpendicular to the coordinate \overrightarrow{PA} , then create bounding lines of line1 and line2 which go trough point P but have an given angle (for example 30 degree) with plane tangent direction and get v shapes of line1-P-line2 . Afterwards, we can obtain 3D volume by rotating V-shapes along the rotation axis \overrightarrow{PA} . After that, we search all candidate points inside that rotation volume using fast KD tree procedure, and finally find the goal point B.

Similarly, we also name \overrightarrow{PB} as the second coordinate.

Step 5. Create an axis (named axis2 in Fig.1) who

is constructed by the cross multiply of $\overrightarrow{PA} \times \overrightarrow{PB}$. Then search all rest candidate points using fast KD tree procedure, and finally find the goal point C according to three conditions of 1) the smallest distance, 2) small enough angle (for example 30 degree, or 60 if the former is not available) between \overrightarrow{PC} and axis2, and 3) not too big angle (for example less than 120 degree) between \overrightarrow{PC} and \overrightarrow{PA} , and \overrightarrow{PC} and \overrightarrow{PB} .

Step 6. calculate the distance from point P to the face ABC in a new constructed tetrahedral element PABC with the expression of

$$d = \frac{\left[(\overrightarrow{PB} - \overrightarrow{PA}) \times (\overrightarrow{PC} - \overrightarrow{PA}) \right] \cdot \overrightarrow{PA}}{\left| (\overrightarrow{PB} - \overrightarrow{PA}) \times (\overrightarrow{PC} - \overrightarrow{PA}) \right|} \quad (2)$$

Note of that equation (2) are using three valid free surface points to calculate the distance.

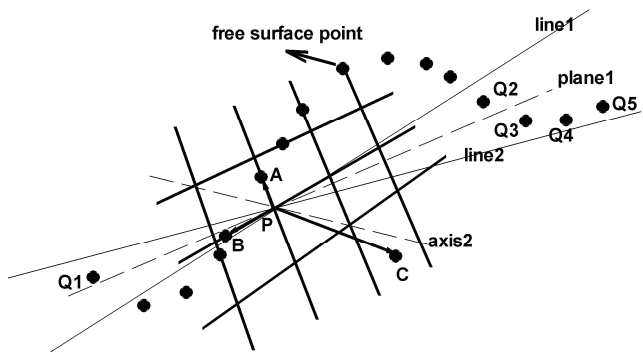


Figure 1 Schematic view of free surface points, close point (P) for KD tree and geometry method for level set reinitialization

The distance can be calculated similarly if there are only one or two valid free surface points found. Also note of that the KD tree have to be rebuilt at each iteration once the free surface points are changing dynamically. Fortunately, the procedure speed of distance calculations for close points is very fast, and the wall-clock time used for this procedure is much smaller than non-linear iteration of rest procedure of level set reinitialization.

After the close points have solved, they will be looked as Dirichlet boundaries to solve the values of other nodes using derivative equations.

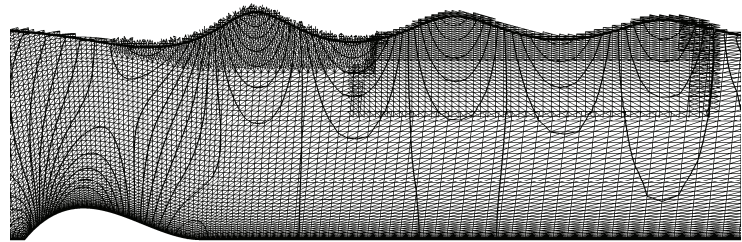


Figure 2 Grid arrangement and pressure distribution

4 Computation examples

4.1 Flow over a submerged body

For this case, Froude number is $Fr=0.426$, the geometry of the 2D submerged body is given by Cahouet^[15], and the submerged body is placed on the bottom of a channel (Fig. 2). In this work, the 2D problem is solved by 3D grid arrangements (3 nodes are arranged into the paper in Fig. 2). Two static overset grids are arranged, one is the hybrid grid of prismatic and hexahedral elements including all physical boundaries, another is Cartesian refinement grid locating at region around second and third waves. The DCI information is communicated to CFD solver through output files for the static overset grids. The detail computational conditions are also introduced in Huang^[5].

The grid arrangement, free surface, and pressure distribution in interesting region are shown in Fig. 2. A comparison between computed free surface elevations and experimental data is presented in Fig. 3, where the results are in good agreement with the experimental data measured by Cahouet^[15].

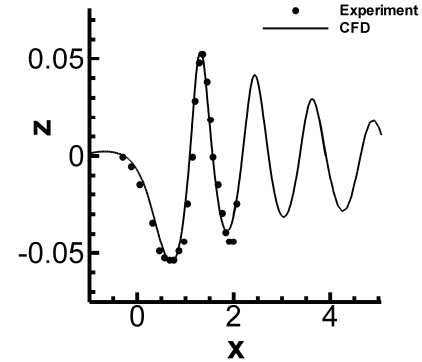


Figure 3 Wave elevation

4.2 Free surface flow around a surface combatant model

Validation studies were also performed on the David Taylor Model Basin (DTMB) model 5512, which is a 3.048m geosim model of DTMB 5415 (5.72m). The computations were carried out for the model advancing in calm water with fixed trim and sinkage. The numerical results were compared with the experimental data measured at the IIHR towing tank by Gui et al.^[16], and Longo and Stern^[17].

Simulations were performed at medium and high speeds corresponding to Froude numbers of $Fr=0.28$ and $Fr=0.41$, and Reynolds numbers of $Re=4.85 \times 10^6$ and $Re=7.10 \times 10^6$, respectively. The double-O and H-type structured grids were used with the total node number of 0.615 million (Huang et al.^[3]).

Fig. 4 shows the time history of the resistance coefficient of water flow on the ship with different conditions.

The results show the resistances are a little bit over predicted, but basically have good agreements with experiment data either for the case of $Fr=0.28$ or $Fr=0.41$. It also can be seen that the solutions of PISO and SST model are better than the one of Projection and BSL models. But note of that the Projection method runs faster than PISO method since the former only runs one iteration for velocity correction.

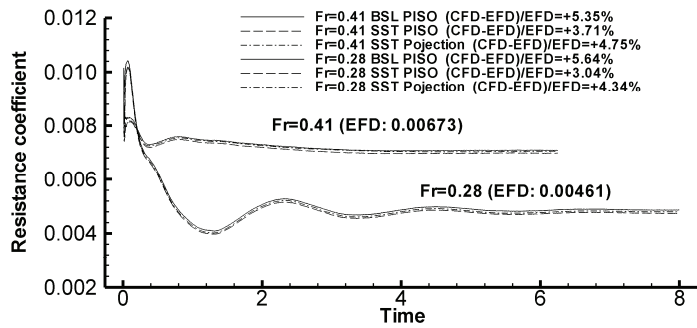


Figure 4 Convergence history of the resistance coefficient

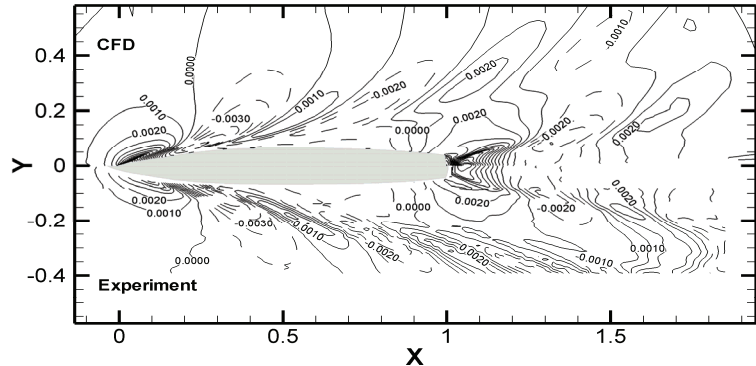


Figure 5 Comparison of wave elevation with experiment data

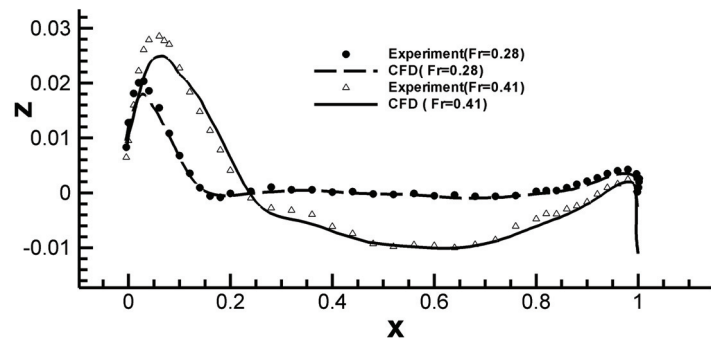


Figure 6 Wave profiles at the hull

A typical Kelvin wave can be observed in Fig. 5 for the case of $Fr=0.28$, where the computational results are also compared with the experimental data. It can be seen that the agreement is good. Fig. 6 presents the wave profiles on the hull surface. The solutions, both for $Fr=0.28$ and $Fr=0.41$ are in good agreements with experimental data. The bow wave was slightly under-predicted, and the solution can probably be improved by using finer grids.

The PIV measurements of the 3D velocity field at the propeller plane $x=0.935$ (the nominal wake) have been reported by Gui et al.

^[16], and Longo and Stern^[17]. Figs. 7 show the comparison of computed axial velocity contours at the propeller plane with the measurements at $Fr=0.28$. There are good agreements between the experimental data and the computational results, and boundary layer is good predicted.

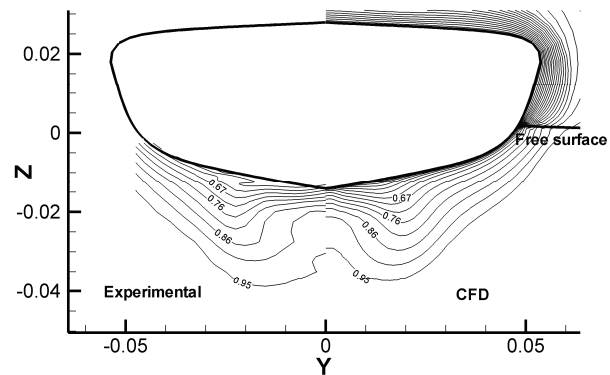


Figure 7 Axial velocity contour at the nominal wake

4.3 Pitch and heave case

Validations are studied for the pitch and heave case on the David Taylor Model Basin (DTMB) model 5512. The numerical results were compared with the experimental data (Irvine et al.^[18], Gui et al.^[19,20]).

Only the case of $Fr=0.28$ (Reynolds number $Re=4.85 \times 10^6$) is studied, with free motions of pitch and heave, and head linear regular wave (wave length: 1.5, wave slop: $ak=0.025$). The coordinate system for computation is created, being static relative to the ship in surge direction, thus the inlet velocity is 1.0 finally. Two dynamic overset grids are used, wherein one is hull grid (fine hexahedral grid: 1.54 million), another is Cartesian background grid (fine hexahedral grid: 1.23 million) used for setting boundary conditions. Three levels of grids of coarse, middle and fine grids are investigated, where the ratio of grid number between two levels is $2\sqrt{2}$. In addition, the time step used is 0.005. For fine grid case, there are total 20

processors used for MPI parallel computation,

Figure 8 Free surface around ship (time=2.5)

wherein 16 processors are arranged for CFD-OHMUGA solver, and 4 processors are arranged for Overset-OHMUGA solver. Different grid partition method is permitted for CFD and overset solvers for parallel computation, and they communicate information directly with related processors (not master and slave mode) in MPI interface. Note of that the time used by Overset-OHMUGA usually can be neglected, since it runs much faster than CFD-OHMUGA solver.

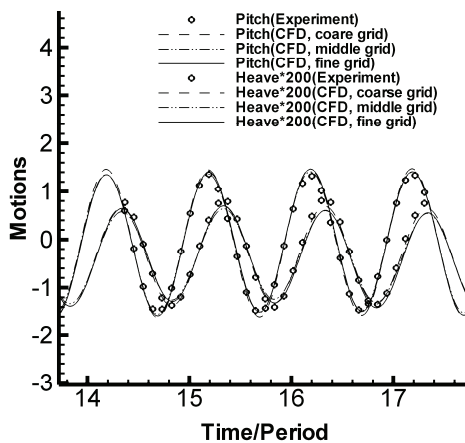


Figure 9 Time history of motions

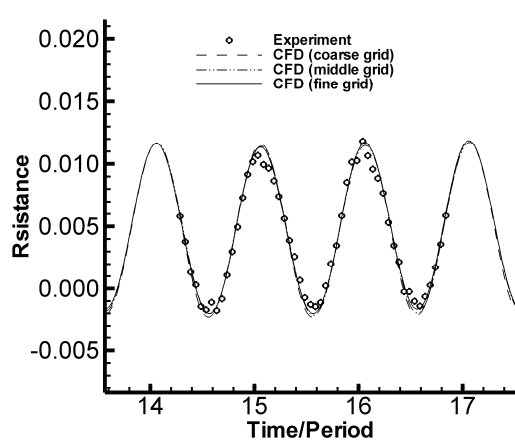


Figure 10 Time history of resistance

Fig. 8 is the free surface around ship at time=2.5. Fig.9 and Fig. 10 show the time history of pitch and heave, and resistance respectively, demonstrating good agreement with experimental data basically. Finer grid looks better for the solutions.

4.4 Course keeping case

Course keeping of DTMB 5512 ship with similar North Atlantic SS5 environment is studied with condition of $Fr=0.28$, $Re=4.85 \times 10^6$ (according to target ship speed). A Bretschneider frequency spectrum with a \cos^2 directional spectrum was used to simulate the incoming linear irregular waves, with a principal direction of Southeast (135°), and most probable wave length of 1.25 (dimensionless), and mean significant wave height of 0.025 (dimensionless). Double propeller of body force model (Hough and Ordway^[21]) is used to control ship speed to the target value, and one active rudder is used to keep ship heading to north direction (rudder is a little bit down from design position to keep enough overlap region for coarse overset grids). Both controllers use PD

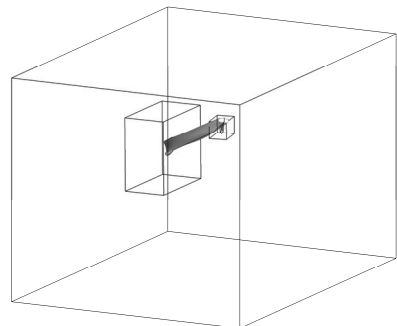


Figure 11 Dynamic overset grid outline

feed back control mode according to errors between current values and target values^[4,11]. There are five coarse dynamic overset grid used of hull (0.625 million), rudder (0.114 million), bow refinement (0.05 million), rudder background (0.065 million), and background (0.167 million) (Fig. 11). All the grids are constructed by hexahedral element for this case.

The simulations are both started with the ship in even keel condition and zero forward speed. An autopilot develops where the ship accelerates to full speed while the controllers operate the rudders and propeller RPM to maintain course and speed.

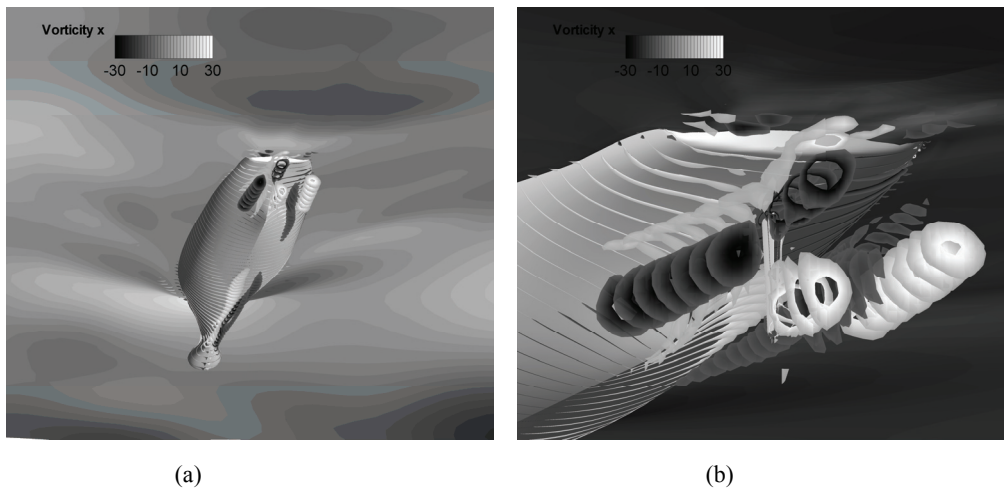


Figure 12 free surface and vortex distribution around ship at time 4.0 (a: bottom view, b: zoom in)

Fig. 12 demonstrates the free surface, vortex and velocity distribution at time=4.0, where we can see the vortex are complicated around ship bottom, especially around the region of propellers and rudder. A pair of vortex with opposite directions appear obviously due to rotations of propellers, meanwhile another pair of vortex appear at top and bottom of rudder. Fig. 13 demonstrates the whole process how the PD controller works for ship speed by active propellers. It shows the history of ship speed and propeller RPS, from which we can see that the ship speed increases with propeller RPS in order to get the target speed, and approximates target speed at about time 4.0, then varies around the target speed. Fig. 14 is the time history of rudder actions, ship rotations and drift, showing that the target heading is well kept by the rudder PD controller at most of time, except around time 5.0 and 9.0 when heading is a little bit big to the west direction. It can be seen that the rudder always adjusts its angle according to errors of current and target headings in order to keep the course, the rudder angle is usually opposite to heading, and its value increases while the heading error increases, and get the maximum values of 15 degree at time about 9.2. Fig. 15 illustrates the ship trajectory during the procedure of course keeping. Although the heading is basically controlled, but there still exist ship drifts and some heading

deviations to west direction during some stages in the history, which explains the trajectory is not always going to north direction, but drifts to west somewhat in the tracked time.

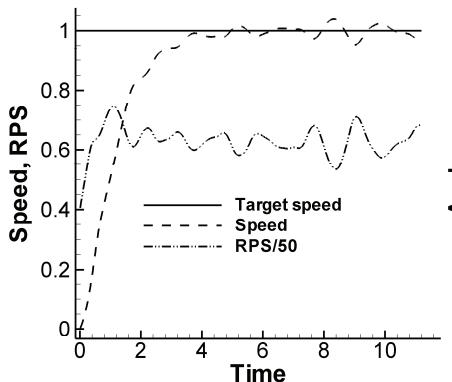


Figure 13 ship speed and propeller RPS

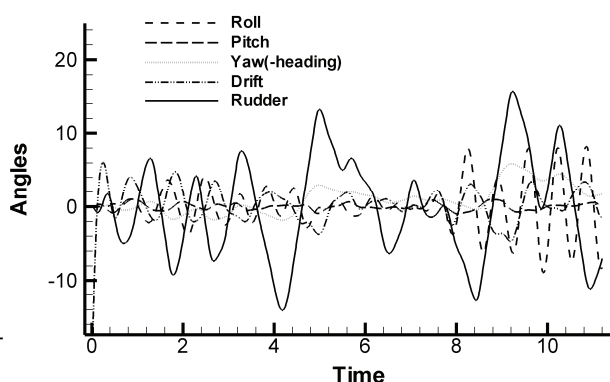


Figure 14 ship motions and rudder angle

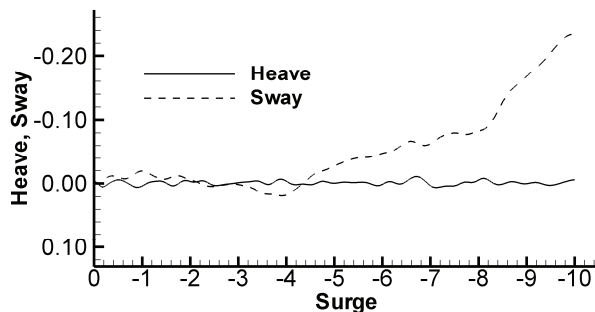


Figure 15 ship trajectory

References

- 1 Osher S, Sethian J A. Fronts propagating with curvature-dependent speed: algorithms based on Hamilton–Jacobi formulations. *Journal of Computational Physics*, 1988, 79:12–49.
- 2 Sussman M, Smereka P, Osher S. A level set approach for computing solutions to incompressible two-phase flow. *Journal of Computational Physics*, 1994, 114: 146–159.
- 3 Huang J, Carrica P M, Stern F. Coupled ghost fluid/two-phase level set method for curvilinear body fitted grids. *Int. J. Numer. Meth. Fluids*, 2007, 55(8): 867-897.
- 4 Huang J, Carrica P M, Stern F. Semi-coupled air/water immersed boundary approach for curvilinear dynamic overset grids with application to ship hydrodynamics. *Int. J. Numer. Meth. Fluids*, 2008, 58(6): 591-624.

- 5 Huang J. An unstructured grid method for free surface turbulence flow in ship hydrodynamics. Proceedings of the Twenty-third International Offshore and Polar Engineering, Anchorage, Alaska, USA, June 30–July 5, 2013, 3: 1011-1018.
- 6 Stern F, Yang J, and Wang Z et al. Computational ship hydrodynamics: Nowadays and way forward. *Int. Ship Building Progress*, 2013, 60(1–4): 3–105.
- 7 Stern F, Yang J, and Wang Z. et al. Recent progress in CFD for naval architecture and ocean engineering. *Journal of Hydrodynamics*, 2015, 27(1): 1–23.
- 8 Vukcevic V, Gatin I, Jasak H. The naval hydro pack: current status and challenges. The 13th OpenFOAM Workshop (OFW13), June 24–29, 2018, Shanghai, China.
- 9 Sethian J A. Fast marching methods. *SIAM Review*, 1999, 41(2): 199-235.
- 10 Carrica P M, Wilson R V, Stern F. An unsteady single-phase level set method for viscous free surface flows. *Int. J. Numer. Meth. Fluids*, 2007, 53: 229–256.
- 11 Huang J. CFD-OHMUGA version 3 user manual 2: mathematical models and numerical methods, OHMUGA Fluid Dynamics Inc., 2019.
- 12 Huang J. Overset-OHMUGA version 1 user manual 2: methods. OHMUGA Fluid Dynamics Inc., 2019.
- 13 Huang J. Iterative band algorithm for hole-cutting for dynamic structured and unstructured overset grid. Proceedings of the Twenty-sixth International Ocean and Polar Engineering, Rhodes, Greece, June 26–July 1, 2016, 3: 368-375.
- 14 Bentley J L. Multidimensional binary search trees used for associative searching. *ACM*, 1975; 18(9): 509-517.
- 15 Cahouet J. Etude numerique er experimentale du probleme bidimensionnel de la resistance de vagues non-lineaire. PhD Thesis, ENSTA, Paris. (in French), 1984.
- 16 Gui L, Longo J, Stern F. Towing tank piv measurement system, data and uncertainty assessment for DTMB model 5512. *Exper. Fluids*, 2001, 31: 336-346.
- 17 Longo J, Stern F. Uncertainty assessment for towing tank tests with example for surface combatant DTMB model 5512. *J. Ship Res.*, 2005, 49: 55-68.
- 18 Irvine M, Longo J, Stern F. Pitch and heave tests and uncertainty assessment for a surface combatant in regular head waves. *Journal of Ship Research*, 2008, 52(2): 146-163.
- 19 Gui L, Longo J, Metcalf B, Shao J. Stern F. Forces, moment and wave pattern for surface combatant in regular head waves part I: measurement systems and uncertainty analysis. *Exp. Fluids*, 2001, 31: 674-680.
- 20 Gui L, Longo J, Metcalf B, Shao J, Stern F. Forces, moment and wave pattern for surface combatant in regular head waves part I: measurement results and discussion. *Exp. Fluids*, 2002, 32: 27-36.
- 21 Hough, G, and Ordway, D. The generalized actuator disk. Technical Report TAR-TR 6401, Therm Advanced Research, Inc., 1964.